General Disclaimer

One or more of the Following Statements may affect this Document

- This document has been reproduced from the best copy furnished by the organizational source. It is being released in the interest of making available as much information as possible.

- This document may contain data, which exceeds the sheet parameters. It was furnished in this condition by the organizational source and is the best copy available.

- This document may contain tone-on-tone or color graphs, charts and/or pictures, which have been reproduced in black and white.

- This document is paginated as submitted by the original source.

- Portions of this document are not fully legible due to the historical nature of some of the material. However, it is the best reproduction available from the original submission.

Produced by the NASA Center for Aerospace Information (CASI)

NF

NASA Technical Memorandum 82640

JT9D Performance Deterioration Results from a Simulated Aerodynamic Load Test

(NASA-TM-82640) JT9D PERFORMANCE DETERIORATION RESULTS FROM A SIMULATED AERODYNAMIC LOAD TEST (NASA) 21 p HC A02/MF A01 CSCL 21E

N81-25012

G3/07 Unclas 26572

Edward G. Stakolich
Lewis Research Center
Cleveland, Ohio

and

William J. Stromberg
Pratt and Whitney Aircraft Group
United Technology Corporation
East Hartford, Connecticut

Prepared for the
Seventeenth Joint Propulsion Conference
cosponsored by the AIAA, SAE, and ASME
Colorado Springs, Colorado, July 27-29, 1981

NASA

JT9D PERFORMANCE DETERIORATION RESULTS FROM A SIMULATED AERODYNAMIC LOAD TEST

Edward G. Stakolich
NASA Lewis Research Center
Cleveland, Ohio

and

William J. Stromberg
Pratt and Whitney Aircraft Group
United Technologies Corporation
East Hartford, Connecticut

E-895

Abstract

This paper presents the results of testing to identify the effects of simulated aerodynamic flight loads on JT9D engine performance. The test results were also used to refine previous analytical studies on the impact of aerodynamic flight loads on performance losses. To accomplish these objectives, a JT9D-7AH engine was assembled with average production clearances and new seals as well as extensive instrumentation to monitor engine performance, case temperatures, and blade tip clearance changes. A special loading device was designed and constructed to permit application of known moments and shear forces to the engine by the use of cables placed around the flight inlet. The test was conducted in the Pratt & Whitney Aircraft X-Ray Test Facility to permit the use of X-ray techniques in conjunction with laser blade tip proximity probes to monitor important engine clearance changes. Upon completion of the test program, the test engine was disassembled, and the condition of gas path parts and final clearances were documented. The test results indicate that the engine lost 1.1 percent in thrust specific fuel consumption (TSFC), as measured under sea level static conditions, due to increased operating clearances caused by simulated flight loads. This compares with 0.9 percent predicted by the analytical model and previous study efforts.

Introduction

The high cost of fuel for aircraft gas turbine engines has resulted in a concerted effort to minimize performance deterioration during the life of an engine. In response to the need for better fuel efficiency, the National Aeronautics & Space Agency initiated the Aircraft Energy Efficiency (ACEE) program in 1975. An element of this program, Engine Diagnostics, managed by the Lewis Research Center investigated the causes and extent of performance deterioration of high bypass ratio turbofan engines. As part of this program, the Pratt & Whitney Aircraft Corp. was awarded a contract to determine the extent and causes of performance deterioration of their JT9D engine. Investigation of historical data[1] on the JT9D engine along with performance data obtained from 32 JT9D-7A engines in the Pan American World Airway's fleet of Boeing 747 SP aircraft[2], have indicated that a performance loss of 0.7 percent cruise SFC occurs in the first few flights of the aircraft. A substantial portion of this loss occurs during flight acceptance testing of the airplane prior to its delivery to the airline and, therefore, is not part of revenue service deterioration. This deterioration is caused by increased operating clearances between rotating fan, compressor and turbine blade tips and their outer air seals. Engine case and rotor deformations result from aerodynamic loads on the engine inlet cowl and inertia loads on the engine which occur during flight. These deformations cause rubbing of the rotating blade tips on their outer air seals (Fig. 1) which produce the increased clearances reducing the efficiency of the engine.

Pratt & Whitney Aircraft Corp. assisted by the Boeing Commercial Airplane Co. has also developed an analytical technique to predict the effects of aircraft flight loads on the performance deterioration of the JT9D engine[3]. This analysis utilizes a NASTRAN finite element model (Fig. 2) of the JT9D engine in a 747 aircraft nacelle.

An aerodynamic load simulation test[4] has been conducted by P&WA in their X-ray test facility to determine the effect of these loads on the performance deterioration of the JT9D engine. The objective of this test program was to determine whether the short term loss in performance was caused by these aero loads or by thrust/thermal loads or by the combination. Blade tip clearance changes were measured with laser proximity probes and X-ray techniques. Using the P&WA component design system, engine and module performance losses were determined from expanded performance instrumentation and results of an analytical teardown of the engine after testing. This paper describes this test program, presents results, and compares these results with the performance deterioration models developed from actual in-service engine data and the NASTRAN analytical model predictions.

Test and Facility Hardware

Engine

The engine used in the test program (JT9D-7AH model) was built from serviceable modules which were flight quality. The modules were assembled with new inner and outer air seals and all gas path seal clearances were set to production blueprint limits. During assembly, all gas path clearances were measured and recorded. Certain engine cases were experimental in order to accommodate the installation of experimental instrumentation. For the test program, the engine was installed in a 747-200 nacelle with a flight inlet to simulate the structural load paths which occur in the flight installation.

Test Facility

The test was conducted in the P&WA production radiographic test stand (Fig. 3). This stand was designed for sea level testing of large high bypass gas turbine engines with airflow rates up to 3000 lb/sec. The stand is equipped with a fully Automatic Production Test Data Acquisition and Control (APTDAC) system, which programs the engine test including the performance of such operations as start-

ing, ignition, bleed valve checks, trimming and limit checks. It provides a continuous display of performance parameters and warning of unacceptable operating parameters. The system records, computes and plots corrected test data and also prints out this data on the engine acceptance documentation.

The engine is mounted to a "hardback" structure which is part of an overhead monorail support system providing automated engine positioning in the test stand. This system is connected to the thrust measuring structure after it is positioned in the test stand.

A unique feature of this facility is its radiographic capability which was utilized for engine internal clearance measurements during the test program. The system is capable of recording internal clearances during engine steady state and transient operations as well as static conditions. An 8-Mev X-ray source is enclosed in a lead vault which is mounted on a gantry that provides five degrees of freedom for positioning the source. Coarse positioning along the engine axis is achieved by a drive chain which moves the entire gantry on casters. Fine positioning is then achieved by moving the X-ray head or the gantry. The X-ray head can be moved in any of the three coordinate directions and can be rotated around two axes providing complete positioning flexibility. The X-ray film in 25 foot rolls is installed in a film holder supported on the test stand floor. A remotely controlled film transport device is used to position successive areas of film in the X-ray beam. This device provides the capability of making up to 24 14x6 inch radiographs at a rate of one every 5 seconds.

Loading Device

The test stand has been modified for the installation of a loading device for the simulation of inlet aerodynamic loads. Loading combinations can be applied at three inlet cowl rib locations through wire cables wrapped around the inlet. The proper combination of load cables pulling at the required angles produces forces and moments on the engine equivalent to the aerodynamic flight load.

The design which has been developed by Pratt & Whitney Aircraft and Boeing is shown in Fig. 4. A loading strap is located at each of the three forward inlet cowl ribs. Each strap is in contact with a rubber strip bonded around the circumference of the cowl. Bonded to each strip is a machined steel ring notched to accept a wire cable, each end of which terminates at a hydraulic jack assembly. The machined steel rings are submerged in polyurethane sheet to provide a smooth aerodynamic surface to prevent turbulent air from being generated and drawn into the inlet from the region of the loading fixture.

Each hydraulic jack assembly contains a jack, a load cell to measure applied load, and an overload protection device which allows the engine to move during transients or an engine stall. The hydraulic jack assemblies are supported by the base and supporting structure.

Jacks are plumbed by pipe and hoses to a hydraulic load maintainer located adjacent to the test stand control room. The load maintainer applies proportional loads to two or more hydraulic jacks simultaneously in response to hand-crank movement. The hydraulic supply to power the maintainer is located conveniently to the maintainer.

Instrumentation

Blade Tip Clearance Measurements

Laser proximity probes were used to obtain clearance changes between the fan, compressor and high pressure turbine blade tips and their outer air seals during engine operation. Nine engine stages were instrumented (Fig. 5) with four probes per stage located circumferentially around each engine case. The actual angular location of each probe was governed by local access to bleed ports to facilitate routing of fiber optic bundles through outer engine case walls. Seven areas in the high pressure compressor, high pressure turbine, and low pressure turbine were X-rayed to obtain both inner and outer airseal clearances (Fig. 5). The low pressure turbine with shrouded blade tips produced good quality X-ray photographs from which blade tip clearances were measured. X-ray photographs of the high pressure compressor and high pressure turbine were used as back-up to the more accurate proximity probe data for determining blade tip clearance changes.

Operation of the probes is based on an optical triangulation system as shown in Fig. 6. Light from a helium-neon laser is focused onto a single 0.001 inch diameter fiber optic. The light is carried along this fiber and emitted from the end of the fiber in the probe, acting as a point source of light. This point source of light is focused by the input lens onto the blades. If the blades are at Position A, the spot of light will be focused by the output lens onto a coherent fiber optic at Point A and, similarly, if the blades are at Position B, the spot will be focused onto Point B of the coherent output fiber. It should be noted that the imaged spot positions at A and B do not depend on the reflectivity of the blades (specular or diffuse, absorptive or reflective), or on the angle of tilt of the blade with respect to the probe. It is a function of only the distance of the blade from the probe. The coherent fiber optic bundle transfers the imaged spot positions from the probe to the video camera. The video camera image is displayed on a video monitor, so that the position of the light spot on the raster of the screen is a measure of the blade clearance. An illuminated reticle is attached to the output fiber optic and serves as a calibration reference for the system. The system is calibrated so that any given position along the scale corresponds to a given blade clearance between the blades and the outer air seal surface.

Data are video tape recorded for permanent record and further analysis of transients. A synchronized digital time/date and engine speed signal are superimposed on the video for reference.

The probe in Fig. 6 is designed for making blade tip clearance measurements through single case structures. It is low in profile and, therefore, can fit into compressor cases underneath vane actuator arms. The probes have high temperature epoxied fiber optics which limit the operating temperature of the fiber optics portion of the probe to 600°F. With a nitrogen purge flow through the probes, they can be operated in temperatures of about 900°F.

Turbine probes have to operate in a consider-

ably more hostile environment, requiring cooling and high pressure seals. Due to the high temperature environment, the blade tips emit radiation which can be picked up by the video system. This "background radiation" is eliminated by using a narrow band-pass interference filter which blocks out all light except for the reflected laser beam light. A folded optical system utilizing a prism at the base of the probe, provides a system that is analogous to the compressor type probe built in a cylindrical form.

The turbine probe is cylindrical so that it can be effectively sealed at the outer case with a piston ring type seal. The probe is bayonetted into the rub strip so that the probe moves with the rub strip, resulting in measurements relative to the rub strip. It is purged with nitrogen for cooling and to keep dirt from accumulating on the probe optics. The temperature vulnerable portion of the probe is the fiber optics which is the part of the probe furthest from the engine flow path.

Engine Performance Measurements

Two data acquisition systems were utilized to obtain engine performance measurements during the test program. The primary system, an Automatic Production Test Data Acquisition and Control (APTDAC) system is normally used for production testing. Measurements are acquired by the system and converted to engineering units. The converted data are used to calculate the required performance parameters and the results are checked to determine out-of-limit conditions. The system is designed to perform real time data acquisition and display the output results on a CRT and a line printer.

Due to the large number of parameters being measured, a portable, High Accuracy Pressure and Temperature Data Acquisition System (HAPTS) was used to support the production data system. The HAPTS has the capacity to record up to 600 bipolar millivolt inputs and 192 pressure inputs on four 48-port scanivalved transducers.

In order to assess module performance deterioration from the test, additional pressures and temperatures were recorded during the test program. The location of the performance instrumentation is shown in Fig. 7.

Engine Case Thermal Measurements

The engine cases were instrumented with thermocouples to measure case temperature variation both axially and circumferentially to correlate axisymmetric and asymmetric thermal closures. Nacelle air temperature and pressure were also measured to determine heat transfer characteristics within the nacelle environment. The locations of this instrumentation are shown in Fig. 8.

The locations of case, flange, and air thermocouples were chosen to determine the impact of engine case metal temperature on adjacent blade tip clearance and for determining the effect of engine external components on the engine's thermal environment.

Test Program

This test program was initiated to provide a better understanding of the relationship between steady state inlet air loads and engine running clearances as well as the effect of these air loads on engine performance deterioration. To achieve these objectives, a test program was developed using a new JT9D-7AH engine in a 747-200 nacelle (as defined under "Test & Facility Hardware"). The engine was ground tested under simulated aerodynamic flight loads during which blade tip clearance, engine performance and thermal data were obtained. The engine was torn down at the completion of the program to measure physical deterioration.

Four flight conditions from the Boeing 747 aircraft flight acceptance test were selected for simulation in this program. These were: take-off, late climb/early cruise, maximum dynamic pressure, and approach. Aerodynamic loads on the inlet cowl at each of these flight conditions were simulated using the strap-type loading device described earlier. The loads were developed by Boeing from analytical and test (wind tunnel and flight) data. These loads were applied to the engine in both a static and a running condition. Fig. 9 shows the predicted inlet air loads compared to the simulated test loads for the take-off flight condition.

The testing was divided into three major parts to satisfy the objectives of the program. The first investigated the effects of thermal and thrust loads on engine running clearances. The second determined the static (non-running) engine response to the applied inlet air loads. The third explored the effect of combined thermal, thrust and inlet air loads on the engine. The testing sequence was determined from the analytical model prediction of blade tip/rub strip interference for the many loading conditions. Loadings which produced no interference were run first and then others were run to produce an increasing level of interference between blade tips and outer seals through the end of testing. This was done so that the wear produced by the smaller loads was not disguised by that produced by the larger loads.

Throughout the test program, power lever movement from one test point to another was limited to 20 rpm/sec or less (N_2 speed) to avoid any transient conditions that might cause blade tip/rub strip interference. Performance data were recorded during all test points to determine which test conditions resulted in performance changes. When a shift in engine performance occurred that was judged to be significant enough to warrant further investigation, a performance calibration run was made. Following is a more detailed description of the testing.

Baseline Clearances and Performance Calibration

After the engine was installed in the test stand but prior to any engine operation, a series of X-rays were taken of the inner and outer gas path seals in the third and fourth stages of the low pressure turbine. These X-rays were taken both at the top (0^{o}) and bottom (180^{o}) of the engine and served as the baseline for any seal wear that might occur during testing. These measurements also served as a calibration of the X-ray system against clearance measurements taken during the analytical build of the engine.

The engine was then motored with the starter to obtain proximity probe clearance measurements at the nine instrumented engine stages. These measurements were compared to those taken during the analytical build of the engine to arrive at a reliable set of

ORIGINAL PAGE IS
OF POOR QUALITY

clearances prior to the start of testing. These clearances were then used as baseline measurements to determine blade tip clearance changes during the test program.

To determine the baseline engine and module performance levels, a baseline calibration consisting of 12 equally spaced power settings was conducted. Each power setting was stabilized for 7 minutes before recording engine and module performance data, engine case environmental data and engine running clearance. Throughout the test program when a significant performance change was indicated, this 12 point calibration run was repeated.

Thrust and Thermal Load Effects

The objective of this portion of the test program was to determine the effects of thrust and thermal loads only on engine blade tip clearances and whether any performance loss occurred due to these loads. The thrust/thermal environment for each of the four flight conditions from the 747 aircraft acceptance test was simulated. Since the test stand is at sea level static conditions, not all of the significant engine parameters could be simulated for the altitude flight conditions. The discharge temperature of the high pressure compressor (T_{T4}) was used as the controlling parameter in setting engine power. To simulate the altitude power setting then, T_{T4} was set as close to the altitude value as possible without exceeding engine thrust, temperature and rotor speed limits.

In addition to the four flight condition test points, clearance and thermal data were also recorded during the baseline performance calibration test to obtain thermal closures between blade tips and outer seals over a wide range of operating conditions. During each test sequence, proximity probe, engine case thermocouple and performance data were recorded simultaneously. X-ray photographs of the low turbine area were also obtained at each test point.

Static Load Effects

Simulated aerodynamic loads as shown in Table I were applied to the engine in a non-running (static) condition using the loading device described previously. Additional loadings of 50 percent take-off, pure vertical, and pure horizontal were also applied.

During each of these loading conditions, the engine was motored with the starter to obtain proximity probe data on the nine engine stages. X-rays of the low turbine area were also obtained at each test load. All strap load values were recorded during the test.

Combined Loads Effect - Thermal, Thrust, and Aerodynamic

The objective of this part of the test program was to determine engine blade tip clearance changes that occur under simulated flight conditions from the combined effects of thermal, thrust and aerodynamics flight loads. A total of 16 combined load conditions were tested including four load levels at each of the four selected flight conditions to be simulated, as shown on Table II. The 100 percent load for each condition represents a typical revenue service flight load. The maximum load for each condition was chosen not to exceed the once-per-5000-flight load level and is less than the engine-nacelle structural limit values so that no damage to engine cases or nacelle cowls would be expected.

A typical test sequence for this part of the program consisted of bringing the engine up to the desired power level and stabilizing for approximately 7 minutes; applying the required simulated aerodynamic load to the inlet through the loading device; then recording proximity probe blade tip clearance data as well as thermal and performance data. An X-ray photograph was also taken at one of the locations in the low pressure turbine. For additional X-ray locations, the load was relieved, and the engine brought to ground idle while the technicians repositioned the X-ray head and film. The engine was then brought back up to power, stabilized, the load reapplied, and an X-ray photograph was taken. This was repeated until all eight locations were X-rayed.

Transient Tests

At the end of the test program, two severe transient power conditions were run with no aerodynamic load simulation. The first consisted of a 10-minute stabilization at full take-off thrust, followed by a rapid deceleration to ground idle, and another 10-minute stabilization. The second transient performed separately from the first was a snap acceleration from ground idle to full take-off thrust after a 10-minute stabilization at ground idle. After reaching take-off thrust, the engine was stabilized at this condition for 10 minutes. Immediately preceeding each transient, proximity probe readings, engine case environment and performance data were recorded. All pretransient measurements were repeated after the 10-minute post-transient stabilization.

Final Performance and Clearance Measurements

At the conclusion of the test program, the 12 point performance calibration was repeated to determine engine and module performance changes. The fan blades were then water washed, and another 12 point calibration was run. A final set of static blade tip clearance measurements were made using both X-ray and proximity probe systems. The engine was motored with the starter to obtain the proximity probe readings. In addition to these final two performance calibration runs, a 12 point calibration was also run after the thrust and thermal load sequence, after each of the combined load flight conditions, and after the transient testing to determine if there were any performance changes caused by these loadings. During the test program, the engine was started 62 times and was run through 86 flight cycles for a total of 147 hours.

Engine Analytical Teardown

After completion of the test program, the engine was disassembled for inspection of hardware deterioration resulting from the testing. Blade tip, and outer and inner air seal wear were measured for all stages. Surface roughness was measured on several fan and compressor blades. Turbine vane bow was also measured to determine flow capacity increase. Other measurements were taken throughout the engine to determine whether there was any distortion that could contribute to engine and module performance changes.

Results

Summary

The test engine lost a total of 1.3 percent in sea level static thrust specific fuel consumption, of which 1.1 percent was due to blade/seal wear. The remaining 0.2 percent was due to the experimental nature of the test program. The results indicate that the inlet aerodynamic loads produce large clearance changes in the fan but have a relatively small impact on clearances in the remainder of the engine. Performance deterioration models developed during previous efforts were updated, based on the results of this test effort. These models relate altitude cruise deterioration, which is approximately 75 percent of sea level take-off performance loss, to revenue service. These updated models confirm that the engine loses 0.7 percent in altitude cruise specific fuel consumption during the airplane flight acceptance test. A more complete discussion of the results is presented in the following paragraphs.

Blade Tip Clearance Changes Due to Thermal Loads

Blade tip clearance changes which occur during engine operation with no external loads applied are produced by internal engine pressures and temperatures, centrifugal forces on rotating blades, and engine thrust. All of these produce axisymmetric blade tip clearance changes except thrust which is reacted off the centerline of the engine. Circumferential thermal gradients around the engine cases can also contribute to nonaxisymmetric clearance changes.

A sample of clearance changes in the fan stage measured with the laser blade tip proximity probes is shown in Fig. 10. These clearance changes include the non-axisymmetric contribution of thrust which is evidenced by a greater clearance change in the lower two quadrants. The same type of information presented in a different manner is shown in Fig. 11 for the third stage of the low pressure turbine. In this case, clearances were obtained from X-ray photographs at the 6 and 12 o'clock positions. The turbine rotor is centered within the case and, as power is increased, the clearance between rotor and case increases. As thrust is increased, the engine bends, causing the clearances at the top of the low-pressure turbine to become tighter on a relative basis and looser at the bottom. The combined effect of case expansion under power and clearance changes from the effect of thrust back bone bending yield these results.

Table III shows the predicted axisymmetric clearance changes versus engine power which were calculated for each stage from the data derived from this portion of the test program. These clearance changes reflect the (axisymmetric) effects of engine rotor speed, gas path temperatures and pressures, engine case temperatures, and nacelle cavity temperatures and pressures. The circumferential nonuniformities whose effects were removed from these clearances are produced mainly by thrust. Although nonuniform case temperatures exist, they contribute essentially no circumferential variation in clearance. These clearance changes from ground idle through take-off power show a decrease for the majority of stages which is to be expected.

Blade Tip Clearance Changes Due to Aerodynamic Loads

Simulated aerodynamic loads were applied to the inlet of the test engine under cold, static conditions to determine the stiffness characteristics of the JT9D-7A engine. The applied loads simulated the inlet pressure distributions of approach (Condition 113), climb/cruise (Condition 104), maximum dynamic pressure (Condition 108), and take-off (Condition 101) from the Boeing 747 Flight Acceptance Test.

Results of the analysis of the proximity probe data are shown in Table IV. Only the fan experienced significant clearance changes; core clearances usually changed by less than 0.005 inch with 0.012 inch being the maximum change. The clearance changes shown reflect only those due to the applied inlet aerodynamic moment, and thus do not include the effect of engine thrust.

The reported clearance changes follow expected trends for the various flight load conditions. Fig. 12 illustrates a typical JT9D engine backbone bending plot for an upward moment about the engine centerline that is in approximately the same direction as the moments for flight conditions 113, 104, and 101. The plot illustrates how the cases and rotors deflect. The clearance changes are simply the difference in deflection between the rotor and case at each engine stage. As can be seen, the greatest clearance changes in the high-pressure compressor should occur in the middle of the module. The values in Table IV confirm this trend. The fan, as previously mentioned, is the module where the largest clearance changes resulting from aerodynamic loading were recorded. The values reported follow the expected trends within probe accuracy.

The X-ray data for the fourth stage low pressure turbine indicate that the blade tip knife edges were either imbedded in the outer air seal or touching the outer air seal during the static load testing. Fig. 13 shows a plot of X-ray data at the 6 and 12 o'clock locations which illustrates this interference.

Blade Tip Clearance Changes Due to Combined Thermal, Thrust, and Aerodynamic Loads

Simulated aerodynamic loads were applied to the inlet of the test engine at stabilized power settings to simulate the combined effects of thermal, thrust, and inlet pressure loads on engine running clearances and performance. The same inlet load conditions applied during static loads testing were used in the combined loads testing. However, the engine was tested over a range of load levels, generally from 50 to 150 percent of the loads that occur in the Boeing 747/JT9D Flight Acceptance Test. The power levels at which the engine was stabilized were the same as those used in the thermal loads testing.

Combined load results from the analysis of proximity probe data for the 100 percent loads levels are presented in Table V. As static test results indicated, only the fan experienced large clearance changes under flight loads. The largest core changes occur in the first high-pressure turbine stage (0.018 inch) and ninth high-pressure compressor stage. Most measured changes in the core, however, were less than 0.005 inch. The clearance changes shown reflect engine bending due to both

thrust and inlet moments. The clearance changes in the low pressure turbine based on X-ray data are shown in Table VI. These clearance changes obtained from the X-ray data analysis reflect the average clearance change for each load type under the average load.

Transient Test Results

In general, the clearance changes measured during the two transient tests were as expected. The performance calibration test which was run after the transient testing revealed no performance loss due to the transient test.

Engine Teardown Results

At the completion of the test program, the engine was disassembled and hardware condition was documented. Measurements taken during the build of the engine were repeated at teardown and included blade tip clearances, gas path inner air seal clearances, seal land wear locations and depths, airfoil surface roughness, and turbine airfoil flow areas. Hardware condition was then evaluated to determine its impact on engine and module performance.

Clearance changes from engine build measured during teardown are shown in Table VII for all blade tip seals. Changes were observed in almost every stage of the engine, with the largest changes being in the fan, the second stage of the high-pressure turbine, and the fifth stage of the low-pressure turbine. In the cold section, these clearance changes were a result of outer air seal wear. In the turbines, they were a result of both blade length loss and gas path outer seal wear.

Seal land wear patterns observed during the teardown of the test engine are shown in Fig. 14 for the fan. The locations of wear were as expected. Wear in the upper left quadrant was produced by the maximum dynamic pressure air load which pulled the fan case down and to the right. The take-off air load pulled the fan case up to the right and produced wear in the lower left quadrant of the fan outer air seal.

The volume of seal material worn from each seal land in the test program was determined for the blade tip seals. Because the seals were new and unworn when the engine was built, the wear volumes were calculated from wear depth, width, and arc length measurements taken at teardown. These wear volumes do not include material removed from blade tips in the turbine section of the engine.

The effects on engine performance of blade tip and gas path inner air seal tip clearance changes, surface roughness increases, and vane bow were assessed using the Pratt & Whitney Aircraft component design system. These effects are shown in Table VIII. The high-pressure compressor and turbine contributed the most to engine performance deterioration, with the single most important factor being the blade tip clearance change in the high-pressure compressor. The increase in blade tip clearances accounted for 1.1 percent of the 1.3 percent total performance loss. The remaining 0.2 percent was caused by surface contamination of airfoils and thermal distortion of high pressure turbine components. These latter two deterioration mechanisms were due to the experimental nature of this program and are not typical of early revenue service. Even though clearance change in the fan was much greater than that in the high pressure compressor and high pressure turbine, the influence coefficients relating change in TSFC to change in clearance are greater for both the high pressure compressor and high pressure turbine than for the fan, which accounts for the results shown in Table VIII.

Performance Analysis

The overall engine performance changes and the component performance changes during the course of testing were determined from calibrations of the engine and from the analytical teardown of the engine at the end of the program. Calibrations were run prior to the application of any loads (base-line calibration), after each series of load applications, after a series of snap transients, and, finally, after the fan blades were washed at the end of the program.

The loss in engine performance from the baseline calibration to the end of the program was 1.3 percent in thrust specific fuel consumption (TSFC). Some performance loss was noted when the simulated climb and approach loads were applied and after the simulated maximum dynamic pressure loads were applied. The major performance loss, however, occurred when the loads which simulated take-off rotation were applied. Washing the fan blades produced a performance improvement in 0.1 percent. Table IX summarizes the engine performance loss throughout the test program.

A comparison of the data obtained during the final engine calibration with the baseline calibration was made, and an analysis was conducted to estimate how much each module's degradation contributed to the 1.3 percent loss in thrust specific fuel consumption. Component efficiency and flow capacity changes were expressed as losses in thrust specific fuel consumption with the aid of the mathematical simulation of the engine. The assessment of performance loss for each module based on engine teardown results was obtained from measurements of rubs, clearances, and airfoil surface roughness in the compression section of the engine and measurements of rubs, clearances, and airfoil and platform distortion in the turbine section. These measurements and the estimated impact on the performance of each component are summarized in Table X which compares the teardown and performance assessment results.

The comparison in Table X shows that the high and low-pressure turbine losses indicated by engine test data agree very well with the teardown results. The total compression section loss indicated by the test data also agrees with that estimated from the teardown measurements. However, the distribution of the loss among the fan, low pressure compressor, and high-pressure turbine differs somewhat as determined by the two methods. Smaller fan and low-pressure compressor losses and a larger high-pressure compressor loss are indicated by the teardown measurements.

Model Refinements

One of the major objectives of this and previous tasks of the JT9D Engine Diagnostics Program has been the development and refinement of analytical models of JT9D engine performance deterioration. This Simulated Aerodynamic Loads Test Program provided the opportunity to investigate the causes of

short term performance losses and to develop the data with which to modify previous analytical studies and predictions.[3] These analytical predictions, combined with the measured performance losses that occurred during the test program, permitted refinement of the individual models for module as well as engine performance deterioration versus flight cycles developed previously under the JT9D Engine Diagnostics Program (Refs. 1 and 2).

A brief description of the analytical model of performance deterioration caused by flight loads is presented below:

A computer simulation of the flight acceptance profile incorporates the proper combination of nacelle loadings, engine thrust, inertia and gyroscopic effects, and engine baseline clearances between blade tips and outer air seals. Exposure to thrust and maneuver loads at each flight condition results in deformation of propulsion system structural members and leads to relative motion between static and rotating components of flow path seals (this is termed closure). These closures are calculated using a NASTRAN model of the JT9D-7 propulsion system. If the motions are larger than can be accommodated by the available clearances, rubs and wear (of blade tips and seals) will occur and result in increased operating clearances. Abradability factors determine the trade off between blade tip and rub strip wear. Performance influence coefficients for each engine stage are then used to determine the performance loss due to the increased operating clearances.

As a result of the data obtained during this test program, revisions were made to all elements of the analytical model to improve the prediction of performance loss caused by flight loads. The updated model was then used to predict the performance loss for this simulated aerodynamic load test program. This predicted loss due to seal wear of +1.1 percent TSFC shows excellent agreement with the +1.1 percent measured loss from the test program. Table XI shows a comparison of rub strip wear predicted by the model for each stage of the engine and measured wear from the test program.

Engine and module performance deterioration models were developed and refined as new data became available from the various tasks within the Engine Diagnostics Program. These models relate the engine performance loss in percent cruise thrust specific fuel consumption and change in exhaust gas temperature to engine flight cycles from the first flight through 3000 flights. All of the contributors to performance loss are included in the models; clearance increases due to flight loads and erosion, surface roughness, and thermal distortion of hot section parts. Fig. 15 shows engine performance losses through 2000 flights updated with the results of this aerodynamic load simulation test program. The model reflects refurbishment of the high pressure turbine every 1000 flights.

Concluding Remarks

The testing and analytical teardown of the JT9D-7AH test engine have significantly improved the understanding of short term engine performance deterioration. The overall thrust specific fuel consumption change was measured to be +1.1 percent which was the result of load induced clearance changes, primarily those resulting from application of the take-off load. The analytical teardown of the test engine showed clearance changes in all modules with the major changes occurring in the fan, high-pressure compressor, and high-pressure turbine.

The rub patterns that occurred in the test engine were compared with both analytical model predictions and those rub patterns documented to have occurred in an engine removed from revenue service. In general, the comparison indicates good agreement in most of the engine stages.

The JT9D performance model refined as part of this effort indicates that the flight inlet aerodynamic loads do not substantially contribute to airplane revenue service performance changes, because much of the deterioration caused by these loads occurs during airplane acceptance testing prior to the start of revenue service. This performance increment should not be considered when comparing cruise performance losses with revenue service usage.

Loads testing of the type conducted under this program should be considered on all new engines or engine/nacelle combinations very early in their development. This early testing would provide the longest possible lead time for refining the total propulsion system design. Analytical studies such as those conducted under earlier phases of the Engine Diagnostics Program, and refined under this phase of the program, are considered to be an important element in the preliminary and detailed design of advanced engines and nacelles.

References

1. Sallee, G. P., "Performance Deterioration Based on Existing (Historical) Data; JT9D Jet Engine Diagnostics Program," Pratt and Whitney Aircraft Group, East Hartford, CT, PWA-5512-21, Apr. 1978. (NASA CR-135448.)

2. Olsson, W. J. and Sallee, G. P., "Performance Deterioration Based on In-Service Engine Data; JT9D Jet Engine Diagnostics Program," Pratt and Whitney Aircraft Group, East Hartford, CT, PWA-5512-35, Apr. 1979. (NASA CR-159525.)

3. Jay, A. and Todd, E. S., "Effect of Steady Flight Loads on JT9D-7 Performance Deterioration," Pratt and Whitney Aircraft Group, East Hartford, CT, PWA-5512-24, June 1978. (NASA CR-135407.)

4. Stromberg, W. J., "Performance Deterioration Based on Simulated Aerodynamic Load Tests, JT9D Jet Engine Diagnostics Program," Pratt and Whitney Aircraft Group, East Hartford, CT, PWA-5512-75, 1981. (NASA CR-165297.)

TABLE I. - SIMULATED AERODYNAMIC LOADING

[Four flight points: thrust, aerodynamic loads.]

	Approximate thrust, lb	Aerodynamic load moment[a] at "A" flange, in-lb
Takeoff	46 000	356 288
Approach	6 700	190 670
Late climb/early cruise	29 000	65 881
Maximum dynamic pressure	43 000	232 234

[a]100 Percent of first flight load.

TABLE II. - COMBINED LOAD TEST CONDITIONS

Four load levels for each condition

Takeoff, percent	25	50	75	100
Late climb/early cruise	50	100	120	140
Maximum dynamic pressure	50	75	100	150
Approach	50	75	100	150

100 Percent is typical revenue service flight load.

TABLE III. - THERMAL LOADS TESTING PREDICTED AXISYMMETRIC CLEARANCE CHANGES VERSUS POWER

[Clearance change in mils from ground idle.]

Stage	Ground idle	Approach	Climb/ cruise	Max. Q	Take-Off
Fan	0	-5	-28	-69	-72
LPC					
2	0	-4	-25	-36	-40
3	0	-2	-11	-17	-19
4	0	-3	-20	-30	-33
HPC					
5	0	-5	-16	-21	-22
6		-5	-18	-23	-25
7		-4	-16	-20	-21
8		-5	-18	-23	-25
9		-6	-14	-19	-20
10		-3	-10	-14	-14
11		-2	-8	-10	-10
12		-1	+1	+3	+3
13		-3	-8	-12	-12
14		-2	-8	-11	-11
15		-3	-10	-13	-14
HPT					
1	0	-6	-21	-24	-25
2	0	-9	-26	-30	-32
LPT					
3	0	-11	-9	-5	-1
4		-2	-25	-22	-21
5		-?	-36	-42	-46
6		-	-34	-41	-45
Relative rotor speed changes:					
N1 rpm	0	341	1596	2100	2234
N2 rpm	0	605	1848	2295	2390

TABLE IV. - CLEARANCE CHANGES DUE TO AERODYNAMIC LOADS

APPLIED TO THE STATIC ENGINE

[Based on proximity probe data.]

Stage	Probe no.	Circumferential location (rear view), deg	Condition[a] - 100 percent load			
			113	104	108	101
			Clearance change, inch			
Fan, stage 1	1	60	+0.029	+0.016	-0.001	
	2	150	-.019	-.006	+.019	-0.041
	3	240	-.040	-.009	0	-.065
	4	330			-.025	
Low-pressure compressor, stage 4	5	77	+0.003	+0.003	+0.003	+0.003
High pressure compressor, stage 5	9	96	+0.001			
	11	276	0	0	-0.001	0
	12	349	0	+0.001		+0.001
High-pressure compressor, stage 9	17	47	+0.001	+0.003	+0.006	0
	18	133	0	-.001	-.003	+0.002
	19	191				
	20	313	+0.003	-0.001	+0.005	+0.001
High-pressure compressor, stage 10	21	60	-0.007	-0.003		
	22	135	-.002	+.010	-0.007	0
	23	192	+.003	+.002	-.001	+0.005
	24	315	+.001	0	+.004	-.001
High-pressure compressor, stage 11	25	75	-0.006	-0.004	-0.005	-0.007
	26	165	0	-.001	-.007	+.001
	27	248	0	-.003	-.005	+.001
	28	345	-.003	-.001	+.003	-.005
High-pressure compressor, stage 14	30	121	-0.002	-0.003	-0.006	0
High-pressure turbine, stage 1	33	60	+0.006	+0.003	+0.006	+0.005
	34	150	+.006	+.004	+.011	+.003
	35	230		+.006		
	36	330		+.012	+.004	

[a]Flight condition descriptions:
No. 113 approach for landing
No. 108 airplane maximum dynamic Pressure
No. 104 late climb/early cruise
No. 101 take-off rotation

TABLE V. - CLEARANCE CHANGES DUE TO AERODYNAMIC LOADS APPLIED TO THE RUNNING ENGINE

[Based on proximity probe data - from no load power condition.]

Stage	Probe no.	Circumferential location (rear view), deg	Condition[a] - 100 percent load			
			113	104	108	101
			Clearance change, inch			
Fan, stage 1	1	60	+0.042	+0.016	-0.006	+0.044
	2	150	-.022	-.010	+.064	-.040
	3	240	-.055	-.008	.004	
	4	330		+.016	-.070	+.034
Low-pressure compressor, stage 4	5	77		+0.003	+0.001	
High-pressure compressor, stage 5	9	96	+0.002	+0.001	+0.002	+0.002
	10	198			+0.007	
	11	276	+.002	+0.001	-.001	+0.002
	12	349	+.001	-.001		-.004
High-pressure compressor, stage 6	14	81		+0.001	0	+0.005
	15	215		0	+.004	
High-pressure compressor, stage 9	17	47	-0.006	-0.003	+0.002	-0.016
	18	133	+.004	+.002	-0.003	-.005
	20	313	-.002	-.004	+.002	-.006
High-pressure compressor, stage 10	21	60	-0.008	-0.003	+0.002	
	22	135	-.001	0	-.010	-.002
	23	192	+.006	0	-.005	-.006
	24	315	+.003	0	+.004	-.002
High-pressure compressor, stage 11	25	75	-0.006	+0.001	-0.002	-0.007
	26	165	+.003	+.004	-.005	+.003
	27	248	+.009	+.009	+.003	+.004
	28	345	-.005	0	+.007	-.005
High-pressure compressor, stage 14	30	121	+0.007	+0.009		0
High-pressure turbine, stage 1	33	60	+0.013	0	-0.005	-0.002
	34	150	+.007	-.006	+.005	-.004
	35	230			0	-.018
	36	330		+.006	-.006	+.006

[a]Flight condition descriptions:
No. 113 approach for landing
No. 108 airplane maximum dynamic Pressure
No. 104 late climb/early cruise
No. 101 take-off rotation

TABLE VI. - LOW PRESSURE TURBINE BLADE TIP CLEARANCE CHANGES DUE TO AVERAGE AERODYNAMIC LOAD ON THE RUNNING ENGINE

[X-ray results.]

Condition[a]	113	104	108	101
load, percent	93.5	102.5	93.5	100
3rd Stage				
12 o'clock	+1	+6	+19	-12
6 o'clock	-2	+3	-18	+2
4th Stage				
12 o'clock	-5	-6	-4	+1
6 o'clock	+4	+7	-21	+16

Clearance changes are in mils from the no-aero-load-at-power condition

[a]113 - Approach for landing
104 - Late climb/early cruise
108 - Airplane max. dynamic pressure
101 - Takeoff rotation

TABLE VII. - BLADE TIP MEASURED CLEARANCE CHANGES

Module	Stage	Clearance change, in.[a]
Fan	1	0.057
Low-pressure compressor	2	-----
	3	0
	4	.001
High-pressure compressor	5	0.006
	6	.012
	7	.003
	8	.007
	9	.002
	10	.006
	11	.007
	12	.007
	13	.005
	14	.013
	15	.014
High-pressure turbine	1	0.012
	2 front	.040
	rear	.040
Low-pressure turbine	3 front	0.010
	rear	.016
	4 front	-----
	rear	-----
	5 front	.051
	rear	.062
	6 front	.028
	rear	.026

[a]Teardown clearance less build clearance.

TABLE VIII. - TEARDOWN RESULTS - PERFORMANCE CHANGES BASED ON HARDWARE CONDITION

Module	Mechanism	Change in efficiency, point	Change in flow capacity, percent	Change in TSFC,[a] percent
Fan	Blade tip clearance	-0.4	-0.5	+0.1
	Surface roughness	-0	-0	+0
	Fan subtotal =			+.1
Low-pressure compressor	Blade tip clearance	-0.1	-0.4	+0.1
	Inner air-seal clearance	-0	-0	+0
	Surface roughness	-.1	-0	+0
	Low-pressure compressor subtotal =			+.1
High-pressure compressor	Blade tip clearance	-0.8	-1.1	+0.4
	Inner air-seal clearance	-0	-0	+0
	Surface roughness	-0	-0	+0
	High-pressure compressor subtotal =			+.4
High-pressure turbine	Blade tip clearance	-0.5	+0.2	+0.3
	Inner air-seal clearance	-0	+0	+0
	First-stage vane bow	-0	+.6	+.2
	High-pressure turbine subtotal =			+.5
Low-pressure turbine	Blade tip clearance	-0.2	+0	+0.2
	Inner air-seal clearance	-0	+0	+0
	Low-pressure turbine subtotal =			+.2
		OVERALL TOTAL =		+1.3

[a]At sea level, constant take-off thrust.

TABLE IX. - ENGINE PERFORMANCE LOSS FOR VARIOUS FLIGHT LOAD CONDITIONS

Test condition	TSFC at constant thrust, percent
Base line	----
After:	
Climb and approach loads	+0.2
Max dynamic pressure loads	+.4
Take-off loads	+1.4
Snap transients	+1.4
Fan wash (end of program)	+1.3

TABLE X. - COMPARISON OF COMPONENT DETERIORATION ASSESSMENT FROM TEARDOWN RESULTS WITH DETERIORATION ASSESSMENT FROM ENGINE DATA

Component	Change in TSFC estimated from teardown measurements, percent	Change in TSFC estimated from engine test data, percent
Fan	+0.1	+0.2
Low-pressure compressor	+.1	+.2
High-pressure compressor	+.4	+.2
High-pressure turbine	+.5	+.5
Low-pressure turbine	+.2	+.2
Total	+1.3	+1.3

Measured change in TSFC = +1.3 percent

TABLE XI. - ENGINE RUB-STRIP WEAR[a] BY STAGE FOR TEST SEQUENCE

Module/stage	Prediction[a]	Test[a]
Fan	22.75	23.8
Low-pressure compressor:		
Second stage	0.63	1.69
Third stage	1.40	.20
Fourth stage	1.92	----
High-pressure compressor:		
Fifth stage	0.17	0.83
Sixth stage	.32	.35
Seventh stage	.08	.16
Eighth stage	.32	----
Ninth stage	.08	.08
Tenth stage	.07	----
Eleventh stage	.28	.35
Twelfth stage	.09	.07
Thirteenth stage	.18	.36
Fourteenth stage	1.24	1.27
Fifteenth stage	.95	.96
High-pressure turbine:		
First stage	0.13	0.13
Second stage	.39	.83
Low-pressure turbine:		
Third stage	0.19	0.19
Fourth stage	----	----
Fifth stage	.75	.73
Sixth stage	.60	.55

[a]Wear volume (cubic inches).

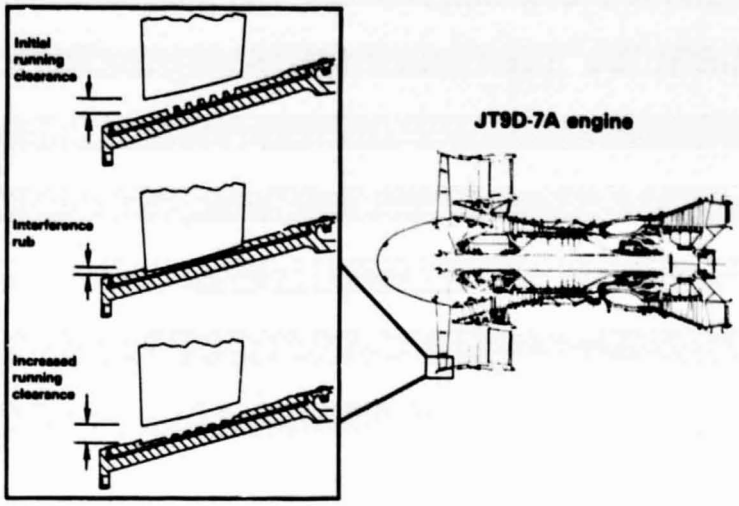

Figure 1. - Effect of aerodynamic flight loads on fan blade tip clearance.

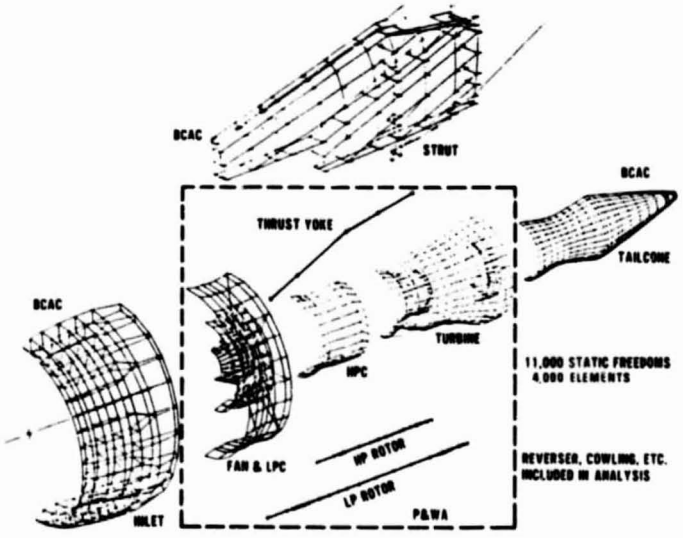

Figure 2. - JT9D-7/747 propulsion system NASTRAN structural model.

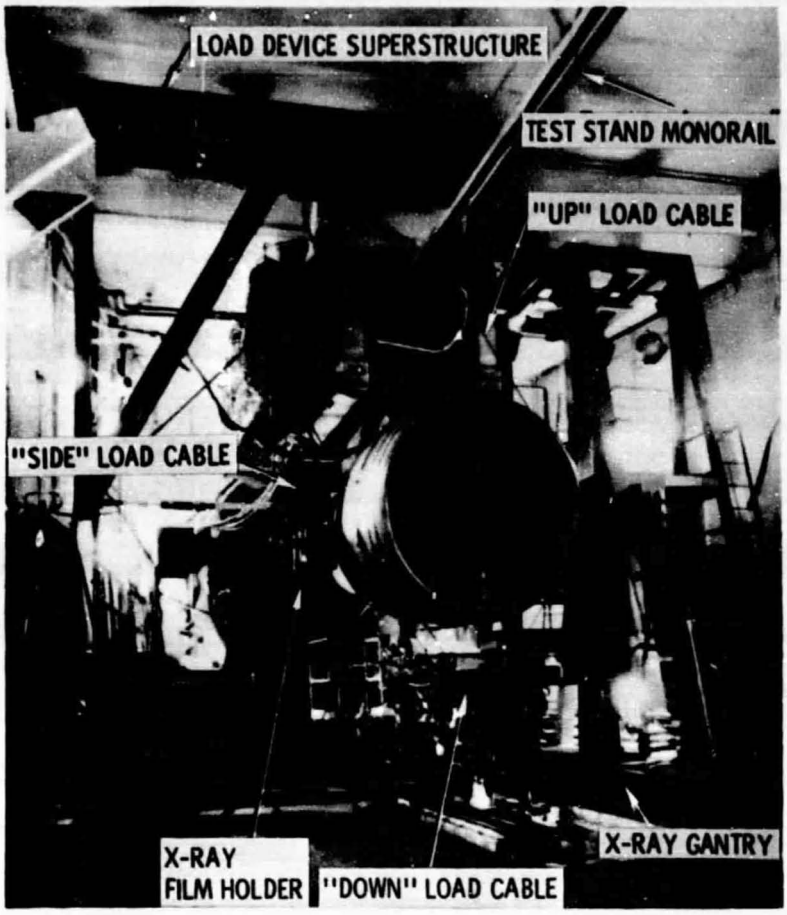

Figure 3. - JT9D-7AH test engine prepared for approach load.

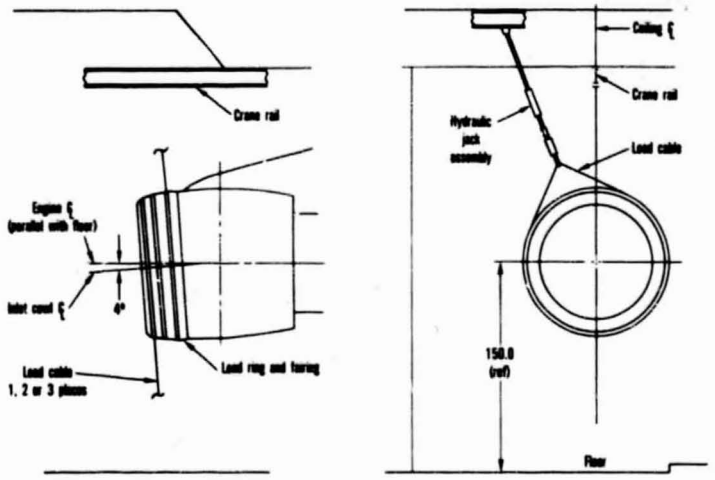

Side view Front view

ORIGINAL PAGE IS
OF POOR QUALITY

Figure 4. - Engine cowl load test set-up.

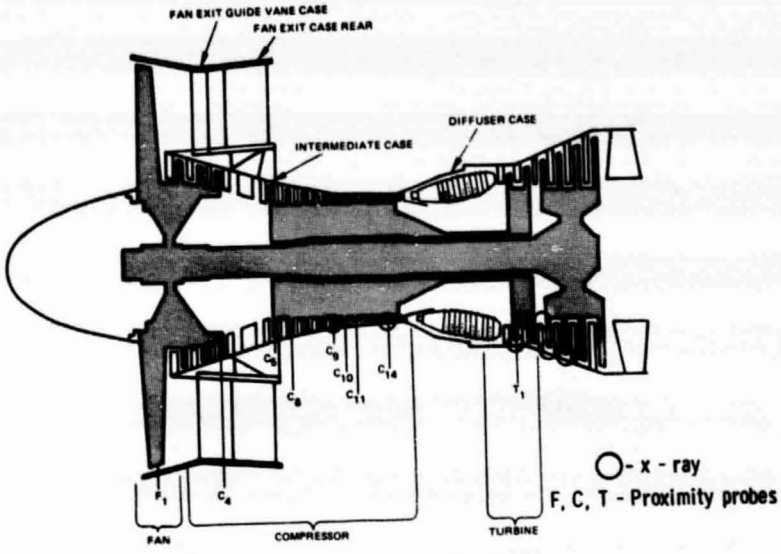

Figure 5. - Proximity probe and x-ray locations.

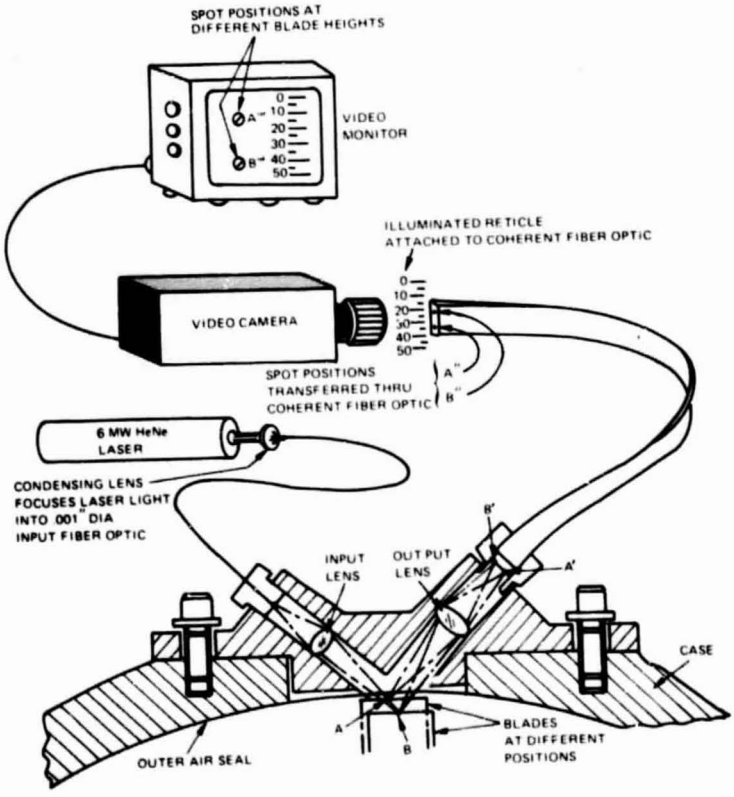

Figure 6. - Laser proximity probe.

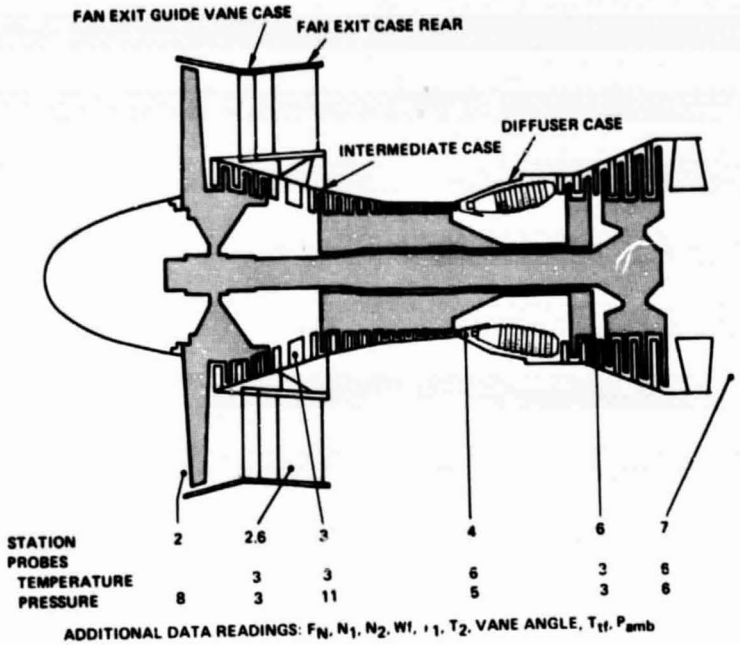

Figure 7. - Performance instrumentation.

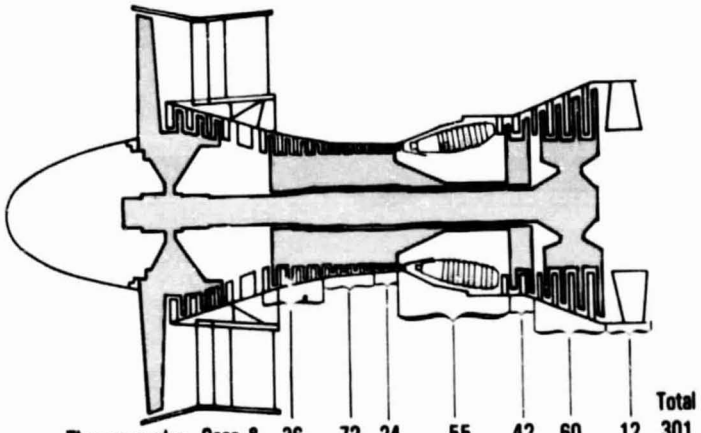

Figure 8. - Thermal load measurements. Thermocouple and pressure instrumentation locations.

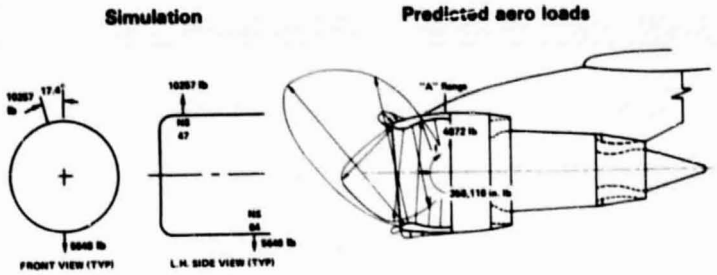

Maximum resultant at "A" flange

	Simulated	Predicted
Moment (in. -lb)	**356,288**	**356,116**

Figure 9. - Inlet air loads. Take-off rotation.

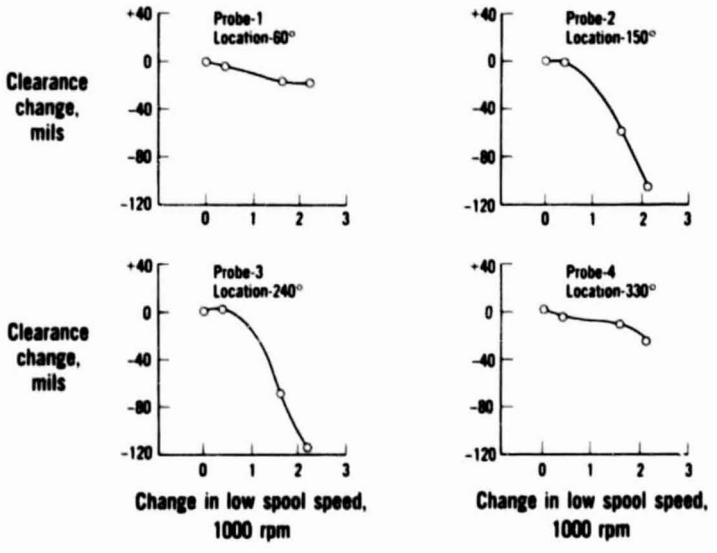

Figure 10. - Fan clearance changes (from ground idle) due to thermal loads - proximity probe data.

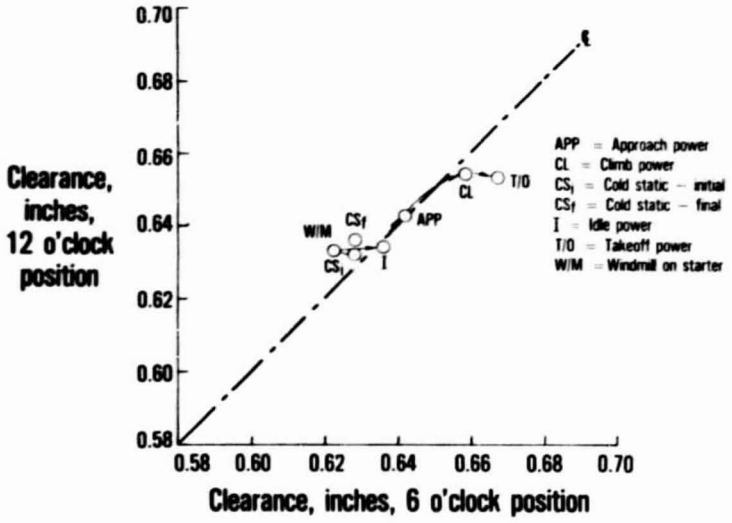

Figure 11. - Third stage low-pressure turbine rear knife edge to case - x-ray results from thermal loads testing.

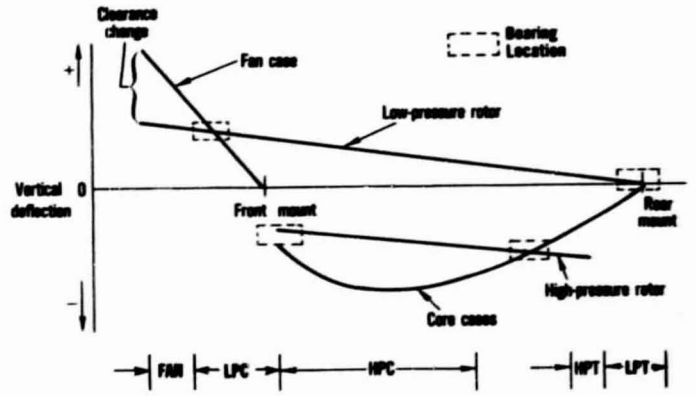

Figure 12. - Typical backbone bending plot for the JT9D engine.

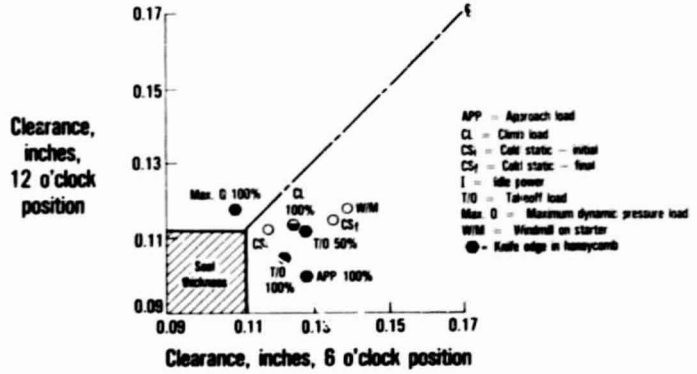

Figure 13. - Fourth stage low-pressure turbine forward knife-edge to outer air seal body - x-ray results from static load test.

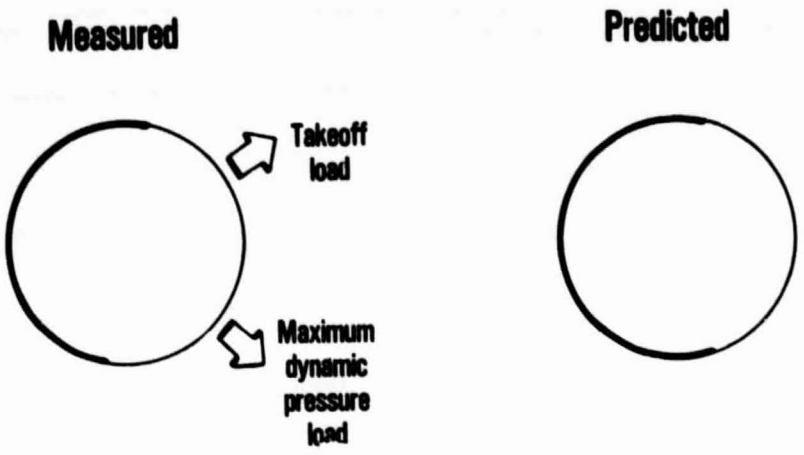

Figure 14. - Predicted versus measured outer seal wear patterns produced by flight loads.

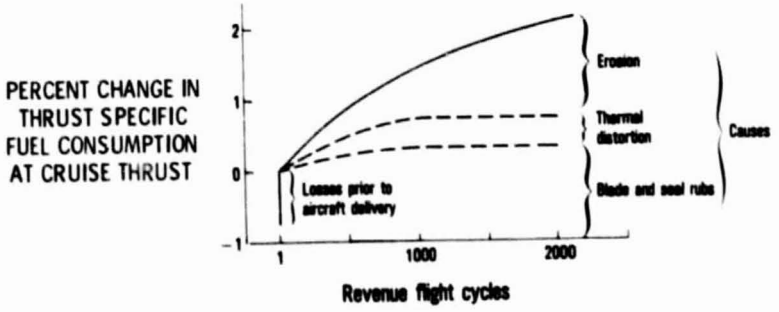

Figure 15. - JT9D perfomance deterioration.

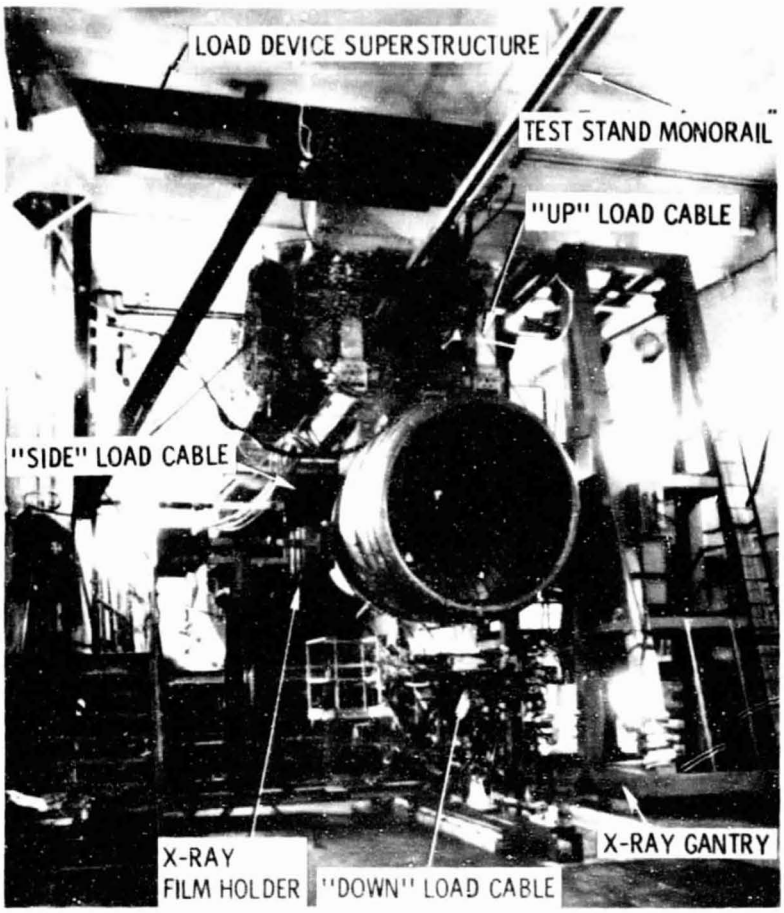

Figure 3. - JT9D-7AH test engine prepared for approach load.

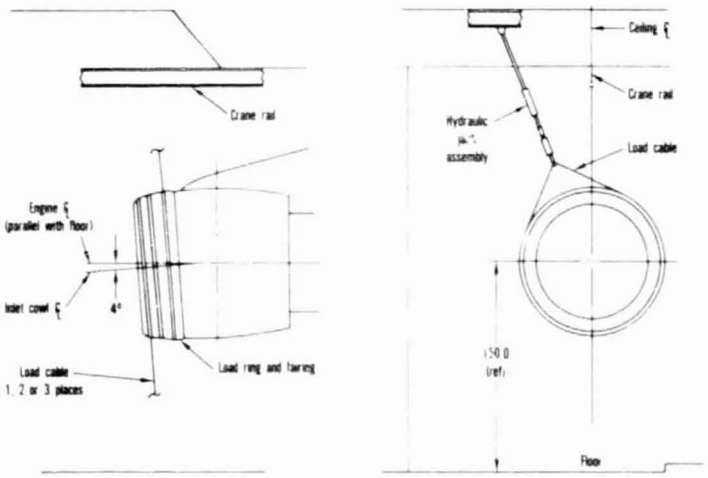

Side view

Front view

ORIGINAL PAGE IS
OF POOR QUALITY

Figure 4. - Engine cowl load test set-up.